Surface Electronic Excited State on Si(100): Structure, Energetics, Lifetime, and Role in Chemical Reactions†

James S. Hess‡ and Douglas J. Doren*

Department of Chemistry and Biochemistry, University of Delaware, Newark, Delaware 19716

Received: March 5, 2002; In Final Form: June 10, 2002

The lowest electronic excited state on the Si(100) surface and its coupling to the ground electronic state have been investigated using first-principles theory. The energy difference between the optimal geometry in the two states is small enough for a significant equilibrium population of the excited state to exist under common reaction conditions. The kinetics of crossing between spin states have been determined by explicit calculation of the minimum-energy crossing point and the spin−orbit coupling between them. The predicted excited-state lifetime is very short, except at low temperature.

Introduction

The Si(100) surface is known to have excited electronic states at an energy much lower than bulk silicon. The bulk has an indirect band gap of 1.17 eV at room temperature. The Si(100) surface gap is also indirect; optical measurements[1,2] find a gap of 0.44−0.64 eV, while photoemission/inverse photoemission[3] or STM[4] measurements find a gap of 0.9 eV (the origins of the differences among these measurements are discussed below). The surface excitation energy is quite sensitive to small changes in surface geometry so that the surface band gap decreases with increasing temperature; at temperatures above 900 K, the surface becomes metallic.[5] Clearly, thermal excitation under common reaction conditions can allow substantial population of surface excited states. In this paper we explore the properties of an excited electronic state on the Si(100)-(2×1) surface and the possible role of this state in chemical reactions.

There are at least two circumstances where excited states may play a role in surface chemical reactions. First, for reactions with activation barriers higher than the surface electronic excitation energy, a reaction path on the excited-state potential energy surface may compete with the ground-state mechanism. For example, in dissociative adsorption of H_2 on Si(100), the measured activation barrier[6,7] of ∼0.8 eV is considerably larger than the lowest electronic excitation energy of the surface, as discussed below. Electronic excitation has been proposed as a possible explanation for the unusual desorption dynamics in this case[8] (though recent evidence suggests that other mechanisms are active at finite coverage[7,9]). Second, in reactions where the reactants and products have different spin states, a nonadiabatic crossing between two different electronic states must occur. An example of this case is silicon surface oxidation by O or O_2 (on either bare or hydrogen-terminated surfaces), where the reactant has a triplet ground state while the adsorbed product is not spin polarized. For such a reaction, two types of mechanism are possible in principle. If the surface site is initially in the singlet ground state, the net spin of the reactants is a triplet and there must be a nonadiabatic singlet/triplet potential energy surface crossing on the reaction path. If the probability of this nonadiabatic crossing is low, the crossing event may be rate limiting. Alternatively, if the reaction path involves a surface site in an (excited) triplet state, antiferromagnetic coupling can give the system a total spin of zero. This latter path avoids the need for a surface crossing during the reaction, at the cost of establishing the initial excitation. By either mechanism, two electronic states are inherently involved in this reaction.

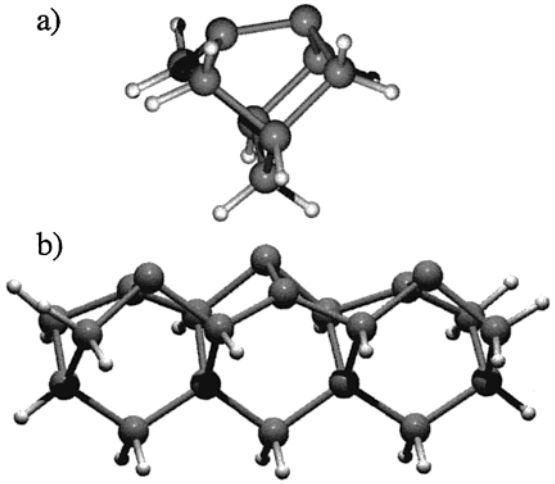

Figure 1. (a) Single-dimer (Si_9H_{12}) and (b) three-dimer ($Si_{21}H_{20}$) cluster models of the Si(100)-(2×1) surface.

In this paper, we make an initial step toward understanding the role of surface electronic excited states by using first-principles theory to explore the lowest excited electronic state on the bare Si(100) surface. This surface has a 2×1 reconstruction that results in a surface dimer structure with one dangling bond per surface atom (Figure 1). The highest occupied orbital on Si(100) can be described as a doubly occupied, π-like bonding orbital between the dangling bonds of a dimer. Within a localized bonding picture, the first excited electronic state is expected to result from an excitation of one electron from this HOMO to the corresponding π^* combination of the dangling bonds. Due to exchange interactions, the spin triplet is lower in energy than the singlet. This implies that the first excited electronic state should have a weaker dimer bond and a wave function of different spatial and spin symmetry than the ground state, so the two states have different reactivity. In particular,

† Part of the special issue "John C. Tully Festschrift".

* Corresponding author. E-mail: doren@Udel.edu.
‡ Current address: Gaussian, Inc. North Haven, CT 06473.

10.1021/jp0206166 CCC: $22.00
Published on Web 07/09/2002

reactions that would formally be forbidden for a symmetric path on the ground state, can be allowed on the excited state.

In the following, we explore the structure and energetics of the lowest excited triplet state on the Si(100) surface using first-principles theory. We study both the equilibrium population of the excited state, and the lifetime of the excited state. The validity of the localized bond picture and the accuracy of our electronic structure methods are both tested. While this paper concerns only the bare surface, our results have direct implications for the possible role of the triplet excited state in chemical reactions. To calculate the kinetics of crossing between electronic states, we have found the lowest energy geometry at which the two states have the same energy (the minimum energy crossing point) and the spin−orbit coupling constant at this geometry. We believe that this is the first time that this approach has been used to predict nonadiabatic transitions between surface electronic states. This methodology will be useful in studying a broad range of localized surface excitations and chemical reactions that involve nonadiabatic events.

Theoretical Methods

Since the excitations of interest are spatially localized, the Si(100) surface was first modeled with a Si_9H_{12} cluster (which contains a single surface dimer; see Figure 1), though calculations were also done with a $Si_{21}H_{20}$ cluster (which contains three surface dimers; see Figure 1) to test the sensitivity to cluster size. Subsurface atoms in the clusters, which would be bonded to other silicon atoms in the extended solid, were terminated with hydrogen atoms. All coordinates in these models were optimized with no constraints, except enforcement of C_s symmetry for the single-dimer model and C_s or C_2 symmetry for the three-dimer models. Most of the calculations reported here are based on density functional theory (DFT), using the hybrid B3LYP functional[10] as implemented in *Gaussian 98*.[11] The 6-311+G(d) Gaussian-type basis set[12] was used on all atoms except the silicon dimer atoms, which were supplemented with extra polarization functions (6-311+G(2df)). All calculations (for both spin states) were performed with spin-unrestricted wave functions. Searches for crossing geometries (at which the two electronic states have the same energy) were done with an algorithm based on that of Bearpark et al.[13] The two surfaces were considered to intersect when the energy difference between them was less than 4×10^{-3} eV.

Tests of some DFT predictions were done by comparing to multiconfiguration wave function methods at specific geometries. These include complete active space self-consistent field theory (CASSCF) calculations. The active space of the wave function consisted of four electrons distributed in four orbitals, specifically the surface dimer σ, σ^*, π, and π^* orbitals (CASSCF(4,4)). In addition, second-order perturbative corrections were applied to these wave functions (CASMP2). These multiconfiguration wave function calculations used the same basis set as the DFT calculations. The spin−orbit coupling constant was calculated with the Z_{eff} approximation using a state-averaged CASSCF(4,4) wave function at a crossing geometry determined using DFT.

Results and Discussion

Geometry and Energetics. We begin with a discussion of predictions from the single-dimer cluster model. A pronounced buckling of the dimer is predicted for the optimized singlet state, in general agreement with the accepted experimental structure.[14] At this ground-state geometry, the calculated energy of the triplet state is 0.79 eV higher than the singlet. However, the optimal geometry in the triplet state is noticeably different. It has an unbuckled structure with an elongated dimer distance (2.41 Å, compared to 2.22 Å for the buckled singlet structure) and is predicted to be 0.34 eV higher in energy than the optimized singlet structure (Figure 2). The free energy difference (calculated with a harmonic model using vibrational frequencies at the two minima) is nearly the same as the energy difference, 0.34 eV at 300 K and 0.36 eV at 800 K. With this free energy separation, approximately 0.5% of the surface dimers will be in this excited state in an equilibrium distribution at 800 K. This population can have a dramatic effect if the excited-state enhances reactions that have very low probability in the ground state.

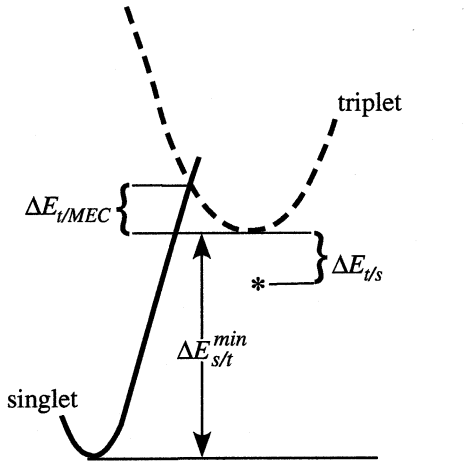

	$\Delta E_{s/t}^{min}$	$\Delta E_{t/MEC}$	$\Delta E_{t/s}$
1-dimer	0.34	0.09	-0.14
3-dimer, C_s	0.40	---	-0.10
3-dimer, C_2	0.38	---	-0.09

Figure 2. Schematic, one-dimensional representation of the singlet and triplet potential energy surfaces, showing the two minima and the minimum-energy intersection of the surfaces. The singlet (solid) and triplet (dashed) curves represent projections along different directions in coordinate space. The only point where the two curves share a common geometry is at their intersection. The asterisk indicates the energy of the singlet state at the optimal triplet geometry. All energies are in eV.

We now address the sensitivity of these energies to the cluster model and the validity of the localized state description. There may be weak electronic interactions between sites that affect the energy and localization of the surface electronic states. Moreover, interdimer interactions tend to stabilize the buckled structure, which may affect the singlet−triplet splitting. To explore these issues, we have determined the singlet−triplet splitting in a three-dimer model, which includes interactions of the center dimer with neighboring dimers in the same row (Figure 1). We did not examine cluster models that included dimers from different rows. The interactions between rows are expected to be small because the interdimer distance in a single row (3.8 Å) is much shorter than that between rows (5.3 Å). This expectation is confirmed by the fact that the surface band states show negligible dispersion (0.1 eV) in the direction ($[01\bar{1}]$) perpendicular to the dimer rows.[15,16] Moreover, DFT calculations on periodic slab models show that the total energy is essentially the same for $c(4\times2)$ and $p(2\times2)$ structures, which differ in the relative buckling of dimers in adjacent rows.[17,18] Finally, the geometry, HOMO−LUMO gap, and activation barrier for hydrogen desorption for this three-dimer model have been shown to agree closely with those of periodic slab models.[19]

We will show that the interactions within a row have a small effect, so there is little reason to examine interactions between rows.

The three-dimer model in the singlet state has C_s symmetry with alternating buckling angles for the dimers (Figure 1). For the triplet state, two models were considered. In both models, the excess spin density is localized on the center dimer, which is again found to be unbuckled (as it was in the single-dimer model). In the first model the outer dimers are buckled in the same direction, giving the cluster C_s symmetry. In the second model the outer dimers are buckled in opposite directions, for overall C_2 symmetry. The relative energetics of the singlet and triplet PES for these two models are summarized in Figure 2. The energy differences between the optimized ground-state structure and the structures optimized in the triplet state are similar to each other, 0.38 and 0.40 eV for the C_2 and C_s symmetry clusters, respectively, and both values are close to the energy difference of 0.34 eV calculated for the single-dimer model. The singlet/triplet energy difference at the optimal triplet geometry is also similar for all three cluster models, with the singlet being 0.14 eV lower than the triplet in the single-dimer model, while in the C_2 and C_s three-dimer models, the singlet is lower by 0.09 and 0.10 eV, respectively. The similarity of these energy differences for the different cluster models supports the conclusions drawn from calculations on the single-dimer model, at least near the optimal triplet geometry. This is the most important case for the conclusions of this paper. However, we have not ruled out the possibility that the triplet state is more delocalized at other geometries (for example, the optimal singlet geometry).

It is natural to question the accuracy of the DFT approach for these calculations, since time-independent DFT is a theory of ground-state energies. However, we are calculating only ground-state properties, since both states are the lowest energy state for a given total spin. Previous work has shown that DFT calculations typically perform well in predicting energy differences between the lowest energy states of different spin, although they are not as reliable for predicting excited states on each spin manifold.[20]

Our predictions can be tested by comparison to experimental results. The Si(100) surface is known to have much lower excitation energies than bulk Si, which has an indirect gap of 1.17 eV at room temperature. The Si(100) surface also has an indirect gap; optical measurements[1,2] find a gap of 0.44−0.64 eV, while photoemission/inverse photoemission[21] and STM[22] measurements find a gap of 0.9 eV. The range of apparent surface excitation energies is partly a consequence of the different physical processes in the measurements. Optical processes produce an exciton in which the energy is lowered by the electron−hole attraction. Processes that inject or extract electrons from the surface have no such stabilizing interaction; they yield a band gap that corresponds to the difference between the surface electron affinity and ionization potential. The optical measurements are most directly comparable to our calculated excitation energies, since both produce an exciton. Selection rules imply that optical excitation must produce a singlet state, which is higher in energy than the corresponding triplet (with the same orbital occupations). Moreover, the optical excitation process does not include geometry relaxation, so that the excited-state energy is higher than the minimum for that state. Thus, these measurements establish an upper bound on the energy difference between the singlet and triplet minima.

A further complication in comparing theory and experiment is the question of which states are involved in the optical excitation. The experimentally observed threshold was originally ascribed to transitions from the bulk valence band maximum, which was thought to be 0.3 eV higher in energy than the π surface state at the Γ point.[1] If we accept this assignment, the measured optical excitation threshold of 0.44−0.64 eV implies a $\pi \rightarrow \pi^*$ excitation energy of 0.74−0.94 eV. This upper bound to the singlet−triplet energy difference is consistent with our results. Of course, substantially higher calculated energy differences would also be consistent with these experiments. On the other hand, more recent measurements[15] and calculations[16] have shown that the surface state is very close in energy to the valence band maximum at Γ. Since a localized $\pi \rightarrow \pi^*$ excited state will be better stabilized by the electron−hole interaction than a bulk$\rightarrow \pi^*$ excited state, it is possible that the localized excitation is lower in energy. If we reinterpret the observed threshold as excitation from the surface state, the measured 0.44−0.64 eV excitation energy is still above our highest calculated value of 0.40 eV, as it must be.

Rohlfing and Louie have done a related calculation on excitations of the Si(111)-(2×1) surface, using the GW approximation.[23] The singlet and triplet excitation energies in that case are similar in magnitude to those that we have found, and the exciton is found to be localized in the surface layer, despite the fact that the occupied surface band is lower in energy than the valence band maximum. In contrast to the excited state that we have studied, Rohlfing and Louie showed that their singlet state was delocalized along the π-bonded chains of atoms on the Si(111)-(2×1) surface. There are several reasons to expect that this reflects fundamental differences in the nature of the electronic states studied, rather than an artifact of either calculation. For example, our calculation focuses on geometries optimized for the triplet state, while Rohlfing and Louie considered only the geometry of the ground state. Thus, their calculation is more relevant to the state resulting from an optical excitation, while our calculation is more relevant to the states reached by thermal excitation. Moreover, the two surfaces have quite different structures, with different coupling along the π-bonded chains of Si(111)-(2×1) than between dimers on Si(100)-(2×1). Finally, triplet excited states (as studied here) are often more localized than singlets (as studied by Rohlfing and Louie).

Excited-State Lifetime. We now turn to the kinetics of crossing from one spin state to the other. The crossing rate is essential for predicting the lifetime of the triplet state, or the kinetic competition between reaction paths involving the two states. A natural experimental test of the role of the triplet excited state would be to excite a nonequilibrium excess population of the triplet. However, the possibilities for establishing such an excess population are constrained by the lifetime of the triplet state.

Thermal excitation (or de-excitation) of an electronic excited state occurs by crossing from one adiabatic potential surface to another at intersections between the surfaces (i.e., at geometries where the two states have the same energy). Potential energy surfaces of different spin symmetry can intersect in an $(n-1)$ dimensional seam, where n is the number of degrees of freedom of the system.[24] The rate of crossing depends on the flux across the seam and the probability to change spin once the seam has been reached. Under equilibrium conditions (and assuming that the crossing probability does not depend strongly on position along the seam), the crossing rate is dominated by the lowest-energy point on the intersection seam, the minimum energy crossing (MEC). We have performed a full optimization of all degrees of freedom in our single-dimer cluster model to find

the singlet/triplet MEC geometry. For the single-dimer model, the calculated MEC geometry is found to be 0.09 eV above the triplet minimum energy (or 0.52 eV above the ground state). The MEC geometry has a nearly symmetric dimer with a dimer bond distance of ~2.54 Å.

If the system reaches the intersection seam between the two spin states, the probability to make a nonadiabatic transition from one to the other depends on the spin−orbit coupling. Using a state averaged CASSCF(4,4) wave function at the MEC geometry described above, we have calculated a spin−orbit coupling coefficient, SOC = 213 cm^{-1}. The crossing probability at the MEC geometry can be estimated with the semiclassical Landau−Zener−Stueckelberg (LZS) approximation.[25] On a single pass across the intersection seam, the probability to cross from one spin state to the other is

$$P_{LZS} = 1 - \exp[-4\pi^2(SOC)^2/h\upsilon\Delta F]$$

where h is Planck's constant, υ is the effective velocity of passing through the crossing point, and ΔF is the difference in slope of the two crossing potential curves in the direction orthogonal to the intersection seam at the MEC. The effective velocity was approximated by the average velocity in a Maxwell−Boltzmann distribution, $\bar{v} = (k_B T/2\pi\mu)^{1/2}$, where μ = 14.04 g/mol is the reduced mass for movement along the dimer coordinate. The difference in slope of the two DFT potential surfaces at the crossing point was found to be ΔF = 0.31 eV/Å. Based upon this analysis, the probability, P_{LZS}, of crossing from the singlet to the triplet state PES at 300 K in a single pass is ~1. This value is not sensitive to modest variations in the parameter values. While the crossing probability is temperature dependent (through the effective velocity) and should decrease slightly with increasing temperature, the fairly large SOC value and the small thermal velocity ensure that the crossing probability is near unity at all temperatures reasonable for a chemical reaction.

We can estimate the energy required for a dimer in the triplet state to cross back to the ground state as $\Delta E_{t/MEC}$, the energy difference between the MEC and the optimized triplet state. Because this energy is only 0.09 eV, it is not large compared to $k_B T$ at room temperature or above and the process is unactivated. The crossing probability at the MEC is close to unity, so the triplet lifetime will be on the picosecond time scale under these conditions. However, at low temperatures the process is activated and we can estimate the equilibrium lifetime of the triplet state in analogy to calculations for other activated rate processes.[26] The flux across the MEC is given by an expression similar to that in the transition state theory of rates, but only a fraction of the molecules at the MEC, given by P_{LZS}, actually cross between surfaces. Thus, the rate for a system at the triplet minimum to cross to the singlet is approximated as

$$k_{t/s}^{cross} = (k_B T/h) \exp[-\Delta E_{t/MEC}/k_B T] P_{LZS}$$

If we apply this analysis at reduced temperature (recognizing that quantum effects will eventually make it invalid), the half-life ($\ln 2/k_{t/s}^{cross}$) for a dimer in the first excited electronic state is ~2×10^{-7} s at 77 K, and the lifetime will increase rapidly with further decreases in temperature. While the short lifetime of the triplet will hinder efforts to create nonequilibrium populations at room temperature, it may be possible to do so at low temperatures. Note, however, that with such a small excitation required to reach the MEC from the triplet minimum, small errors in the calculated crossing energy can have a significant impact on quantitative predictions of the lifetime.

Finally, we have evaluated the possibility that the DFT methods used here may not accurately reflect the balance among various electron correlation effects as a function of geometry and spin state. For example, static (or nondynamic) correlation effects are expected to be important near the MEC geometry where the two spin states have the same energy. The singlet state at the MEC geometry can be described as being intermediate between a singlet diradical and a π-type bond. Previous studies have demonstrated the ability of single-determinant DFT to describe such systems within certain limits.[20] We have tested the agreement between DFT and a wave function method which is more generally able to account for static correlation, namely complete active space self-consistent field theory (CASSCF). This multideterminant wave function method is commonly used in searching for intersections between potential surfaces. The active space of our CASSCF(4,4) wave function in our calculations included configurations of four electrons distributed in the surface dimer σ, σ^*, π, and π^* orbitals. At the MEC geometry optimized using DFT, the singlet/triplet energy difference predicted by a CASSCF(4,4) wave function is only 0.02 eV. Thus, DFT and CASSCF both predict a small energy difference at this geometry, suggesting that DFT has properly accounted for the static correlation at the MEC geometry. While CASSCF is an alternative to DFT in MEC searches, it is not more reliable than DFT since CASSCF neglects effects of dynamic correlation that are accounted for by DFT. To estimate the magnitude of dynamic correlation effects, we have used a perturbative method based on the CASSCF wave function, known as CASMP2. We find a splitting of 0.12 eV at the MEC, again consistent with the DFT prediction that the surfaces are close in energy at this geometry. There is no reason to expect that theories as different as DFT and CASMP2 should predict identical MEC geometries. It is not feasible to search for the MEC with CASMP2 to compare the geometries, nor is CASMP2 necessarily more accurate than DFT. However, if DFT were substantially wrong in accounting for correlation effects and predicting the MEC geometry, the CASMP2 splitting would be much larger. While DFT, CASSCF, and CASMP2 would each predict slightly different geometries and energies for the MEC, all three energy calculations are consistent with an intersection between the surfaces at low energy.

Conclusions

We have shown that a low-lying triplet excited state on the Si(100) surface can have chemically significant equilibrium populations at common reaction temperatures. Using energies estimated from the single-dimer model, about 0.5% of the surface sites would be in the excited state at 800 K. This approximate value should not be regarded as a quantitative prediction, since small errors in the excitation energy will have a large impact on the excited-state population. However, we find little variation in the predicted excitation energy with cluster size. Available experimental data imply that the actual excitation energy could be no more than about 0.2 eV higher than our predicted value.

The lifetime of the excited state at room temperature and above is expected to be very short, though it increases with reduced temperature. This means that kinetic limitations will not prevent an equilibrium population from being achieved. On the other hand, the short lifetime limits the possibilities for direct experimental tests of the role of excited dimers.

This work illustrates how a direct search for the minimum energy crossing point between two electronic states may be implemented for a solid surface. This same approach will be

useful in understanding the kinetics of nonadiabatic surface reactions, such as reactions with molecular or atomic oxygen. While there is no direct evidence of the role played by nonadiabatic transitions, it is clear that they must occur. Theoretical work by Kato et al.[27] has explored the implications of this crossing for O_2 on Si(100), though they were not able to do a search for the crossing point between the surfaces. In cases with higher activation barriers, such as on hydrogen covered surfaces, the importance of accurate searches for surface crossings, as demonstrated here, is likely to be pronounced.

Acknowledgment. This work was supported by the National Science Foundation through grants CTS-9724404 and CHE-9971241, and through computing resources provided by the National Partnership for Advanced Computational Infrastructure at the San Diego Supercomputer Center.

References and Notes

(1) Chabal, Y. J; Christman, S. B.; Chaban, E. E.; Yin, M. T. *J. Vac. Sci. Technol. A* **1983**, *1*, 1241.
(2) Mönch, W.; Koke, P.; Krueger, S. *J. Vac. Sci. Technol.* **1981**, *19*, 313.
(3) Himpsel, F. J.; Fauster. Th. *J. Vac. Sci. Technol. A* **1984**, *2*, 815.
(4) Hamers, R. J.; Köhler, U. K. *J. Vac. Sci. Technol. A* **1987**, *7*, 2854.
(5) Gavioli, L.; Grazia Betti, M.; Mariana, C. *Phys. Rev. Lett.* **1996** *77*, 3869.
(6) Bratu, P.; Kompa, K. L.; Höfer, U. *Chem. Phys. Lett.* **1996**, *251*, 1.
(7) Zimmermann, F. M.; Pan, X. *Phys. Rev. Lett.* **2000**, *85*, 618.
(8) Doren, D. J. *Adv. Chem. Phys.* **1996**, *95*, 1.
(9) Dürr, M.; Hu, Z.; Biedermann, A.; Höfer, U.; Heinz, T. F. *Phys. Rev. Lett.* **2002**, *88*, 46104.
(10) Lee, C.; Yang, W.; Parr, R. G. *Phys. Rev. B* **1988**, *37*, 785. Becke, A. D. *J. Chem. Phys.* **1993**, *98*, 5648.
(11) Frisch, M. J.; Trucks, G. W.; Schlegel, H. B.; Scuseria, G. E.; Robb, M. A.; Cheeseman, J. R.; Zakrzewski, V. G.; Montgomery, J. A., Jr.; Stratmann, R. E.; Burant, J. C.; Dapprich, S.; Millam, J. M.; Daniels, A. D.; Kudin, K. N.; Strain, M. C.; Farkas, O.; Tomasi, J.; Barone, V.; Cossi, M.; Cammi, R.; Mennucci, B.; Pomelli, C.; Adamo, C.; Clifford, S.; Ochterski, J.; Petersson, G. A.; Ayala, P. Y.; Cui, Q.; Morokuma, K.; Malick, D. K.; Rabuck, A. D.; Raghavachari, K.; Foresman, J. B.; Cioslowski, J.; Ortiz, J. V.; Stefanov, B. B.; Liu, G.; Liashenko, A.; Piskorz, P.; Komaromi, I.; Gomperts, R.; Martin, R. L.; Fox, D. J.; Keith, T.; Al-Laham, M. A.; Peng, C. Y.; Nanayakkara, A.; Gonzalez, C.; Challacombe, M.; Gill, P. M. W.; Johnson, B. G.; Chen, W.; Wong, M. W.; Andres, J. L.; Head-Gordon, M.; Replogle, E. S.; Pople, J. A. *Gaussian 98*, revision A.7; Gaussian, Inc.: Pittsburgh, PA, 1998.
(12) McLean, A. D.; Chandler, G. S. *J. Chem. Phys.* **1980**, *72*, 5639. Krishnan, R.; Binkley, J. S.; Seeger, R.; Pople, J. A. *J. Chem. Phys.* **1980**, *72*, 650.
(13) Bearpark, M. J.; Robb, M. A.; Schlegel, H. B. *Chem. Phys. Lett.* **1994**, *223*, 269.
(14) Structural studies have been recently reviewed in Konecny, R.; Doren, D. J. *J. Chem. Phys.* **1997**, *106*, 2426 and Robinson Brown, A.; Doren, D. J. *J. Chem. Phys.* **1998**, *109*, 2442.
(15) Johansson, L. S. O.; Uhrberg, R. I. G.; Måartensson, P.; Hansson, G. V. *Phys. Rev. B* **1990**, *42*, 1305.
(16) Rohlfing, M.; Krüger, P.; Pollmann, J. *Phys. Rev. B* **1995**, *52*, 1905.
(17) Ramstad, A.; Brocks, G.; Kelly, P. J. *Phys. Rev. B* **1995**, *51*, 14504.
(18) Fritsch, J.; Pavone, P. *Surf. Sci.* **1995**, *344*, 159.
(19) Penev, E.; Kratzer, P.; Scheffler, M. *J. Chem. Phys.* **1999**, *110*, 3986.
(20) Brink, M.; Jonson, H.; Ottosson, C.-H. *J. Phys. Chem. A* **1998**, *102*, 6513. Cramer, C. J. *J. Am. Chem. Soc.* **1998**, *120*, 6261.
(21) Himpsel, F. J.; Fauster, Th. *J. Vac. Sci. Technol. A* **1984**, *2*, 815.
(22) Hamers, R. J.; Köhler, U.K. *J. Vac. Sci. Technol. A* **1989**, *7*, 2854.
(23) Rohlfing, M.; Louie, S. G. *Phys. Rev. Lett.***1999**, *83*, 856.
(24) Tully, J. In *Dynamics of Molecular Collisions, Part B*; Miller, W. H., Ed.; Plenum: New York, 1976.
(25) Nakamura, H.; Zhu, C. *Comments At. Mol. Phys.* **1996**, *32*, 249.
(26) Pechukas, P. In *Dynamics of Molecular Collisions, Part B*; Miller, W. H., Ed.; Plenum: New York, 1976.
(27) Kato, K.; Uda, T.; Terakura, K. *Phys. Rev. Lett.* **1998**, *80*, 2000.